

Specific heat and non-linear susceptibility in spin glasses with random fields

M. V. Romitti,¹ F. M. Zimmer,^{1,2,*} C. V. Morais,³ and S. G. Magalhaes^{4,†}

¹*PGFísica, Universidade Federal de Santa Maria, 97105-900 Santa Maria, RS, Brazil*

²*Instituto de Física, Universidade Federal de Mato Grosso do Sul, 79070-900 Campo Grande, Brazil*

³*Instituto de Física e Matemática, Universidade Federal de Pelotas, 96010-900 Pelotas, RS, Brazil*

⁴*Instituto de Física, Universidade Federal do Rio Grande do Sul, 91501-970 Porto Alegre, RS, Brazil*

We study magnetic properties of spin glass SG systems under a random field (RF), based on the suggestion that RFs can be induced by a weak transverse field in the compound $\text{LiHo}_x\text{Y}_{1-x}\text{F}_4$. We consider a cluster spin model that allows long-range disordered interactions among clusters and short-range interactions inside the clusters, besides a local RF for each spin following a Gaussian distribution with standard deviation Δ . We adopt the one-step replica symmetry breaking (RSB) approach to get an exactly solvable single-cluster problem. We discuss the behavior of order parameters, specific heat C_m , nonlinear susceptibility χ_3 and phase diagrams for different disorder configurations. In the absence of RF, the χ_3 exhibits a divergence at T_f , while the C_m shows a broad maximum at a temperature T^{**} around 30% above T_f , as expected for conventional SG systems. The presence of RF changes this scenario. The C_m still shows the maximum at T^{**} that is weakly dependent on Δ . However, the T_f is displaced to lower temperatures, enhancing considerable the ration T^{**}/T_f . Furthermore, the divergence in χ_3 is replaced by a rounded maximum at a temperature T^* , which becomes increasingly higher than T_f as Δ enhances. As a consequence, the paramagnetic phase is unfolded in three regions: (i) a conventional paramagnetism ($T > T^{**}$; (ii) a region with formation of short-range order with frozen spins ($T^* < T < T^{**}$); (iii) a region with slow growth of free-energy barriers slowing down the spin dynamics before the SG transition ($T_f < T < T^*$) suggesting an intermediate Griffiths phase before the SG state. Our results reproduce qualitatively some findings of $\text{LiHo}_x\text{Y}_{1-x}\text{F}_4$ as the rounded maximum of χ_3 behavior triggered by RF and the deviation of the conventional relationship between the T_f and T^{**} .

Keywords: Spin Glasses, Critical Properties, Non-Linear Susceptibility, Replica-Symmetry-Breaking.

PACS numbers: 75.10.Nr, 75.50.Lk, 05.70.Jk, 64.60.De

I. INTRODUCTION

There have been an intense experimental and theoretical debate about the behavior of the non-linear susceptibility χ_3 in the diluted Ising dipolar ferromagnetic compound $\text{LiHo}_x\text{Y}_{1-x}\text{F}_4$ (see, for instance, [1, 2]). This quantity is considered one of the fingerprints of a second order spin glass (SG) transition [3]. In the absence of an applied transverse field H_t , the SG transition in this compound is well captured experimentally by χ_3 that diverges at the so called freezing temperature T_f^0 [4]. Thus, one could expect that the application of H_t would lead $\text{LiHo}_x\text{Y}_{1-x}\text{F}_4$ to behave as a quantum Ising SG [5, 6]. However, it was found that the divergence in χ_3 is smoothed out and replaced by a rounded maximum at a certain temperature T^* lower than T_f^0 . A possible explanation considers random fields (RFs) induced by the coupling between H_t with the off diagonal terms of the dipolar interactions in $\text{LiHo}_x\text{Y}_{1-x}\text{F}_4$ [7, 8]. This mechanism allows to reproduce successfully the experimental behavior of χ_3 [8, 9].

For instance, in the $\text{LiHo}_x\text{Y}_{1-x}\text{F}_4$ for $H_t = 0$, the single ion ground state is a doublet (or equivalently up and down Ising spin states) separated from the first excited state by an energy ~ 9.4 K [10]. For the temperature range of interest, only these two Ising state are significantly populated. This degeneracy is lifted when H_t is turned on, carrying to quantum mechanical mixing of the up and down states. The microscopic hamiltonian of this compound considers basically dipolar interactions [8] that can be projected into these two states resulting in an effective disordered Ising model with an effective transverse field Γ proportional to the energy splitting between the up and down Ising states [11]. Moreover, the off-diagonal terms of the dipolar interactions are not canceled by symmetry in the disordered compound ($x < 1$), generating an effective longitudinal RF which is dependent of H_t . For small intensities of H_t (for instance, $H_t < 0.5T$), the energy splitting of the Ising ground state doublet is negligible¹. Thus, the quantum tunneling between the up and down Ising states can be also neglected [10]. This scenario corresponds to a semi-classical regime. On the other hand, there are experimental results indi-

* fabiozimmer@gmail.com

† sgmagal@gmail.com

¹ This situation refers to the paramagnetic phase.

cating that even for this regime, RF can be already quite active. For instance, Ref. [1] displays not only χ_3 vs H_t but also T^* vs H_t for $\text{LiHo}_{0.165}\text{Y}_{0.835}\text{F}_4$. In the first case, the divergence of χ_3 is clearly replaced by a maximum already for $H_t < 0.2T$. In the same range, T^* is clearly decreasing as H_t is increased.

Very recently, the χ_3 has been theoretically studied using the induced RF mechanism in the quantum [9] and semi-classical regimes [12]. In this last regime, as pointed above, it is considered a weak H_t , enough to induce a RF but not enough to lead the quantum fluctuations dominate the thermal ones. Thereby, the conceptual and mathematical framework of the classical replica mean field theory for SG can be applied [13–16]. In that framework, it is known that in the absence of RF, χ_3 can be directly related with the inverse of the eigenvalue replica λ_{AT} [3]. Thus, χ_3 diverges exactly as $\lambda_{\text{AT}} = 0$ which is the onset of the replica symmetry breaking (RSB) SG phase at the freezing temperature T_f^0 . However, results from Ref. [12] showed that as RF is present the situation is more complex, the relationship of χ_3 with λ_{AT} is changed (see also Refs. [17, 18]). Nevertheless, $\lambda_{\text{AT}} = 0$ still locates the RSB SG transition at T_f (the freezing temperature with RF). Therefore, the divergence found in χ_3 is replaced by a rounded maximum located at T^* which no longer coincides with T_f . In fact, T^* is increasingly higher than T_f but decreases as the RF effects become more important [12]. As a consequence, the paramagnetic phase is unfolded in two regions, with one of them probably being a Griffiths phase [19]. It should be remarked that this phase diagram is basically preserved in the quantum regime [9].

Another probe which can bring information on the $\text{LiHo}_x\text{Y}_{1-x}\text{F}_4$ physics is the magnetic specific heat C_m . It is well known from conventional SG systems that the experimental C_m does not present any sharp anomaly at the SG transition being the critical exponent α negative, around -2 (see Ref. [20] and references therein). Actually, C_m presents a broad maximum around a certain temperature T^{**} estimated to be 20%-40% higher than the freezing temperature [3]. This broad maximum in the C_m located above the SG transition temperature is one of the most important experimental fingerprints of the usual SG behaviour. Interestingly, as for χ_3 , the experimental behavior of specific heat in the $\text{LiHo}_x\text{Y}_{1-x}\text{F}_4$ also has controversies even in absence of H_t . In the extreme dilution limit $x = 0.045$, the debate focused on the question whether exists a spin liquid antighlass as ground state instead of a SG-like state [21]. The antighlass scenario is based on the observation of sharp peaks in the specific heat. In contrast, Quilliam and collaborators [22] observed a broad maximum for the specific heat, as expected for a SG-like state. This debate is a quite clear indication that specific heat is also source of interesting information on the complex physics of the $\text{LiHo}_x\text{Y}_{1-x}\text{F}_4$

². However, not much attention has been given to the behavior of magnetic specific heat in the presence of H_t . Such kind of study can be helpful to complement and clarify the puzzling situation presented by χ_3 behavior described above.

The goal of the present work is to provide an unified analytical description of the behavior of magnetic specific heat and χ_3 of an SG model with the presence of a RF. It is assumed that even weak H_t can induce a RF as proposed by Refs. [7, 8]. Firstly, it should be emphasized that the Sherrington-Kirkpatrick (SK) theory [16], which is the standard mean-field procedure for SG was very successful in explaining many aspects of the experimental behavior of spin glass systems, except, the C_m . Actually, this approach predicts the C_m with a sharp cusp at the freezing temperature. This result is not consistent with the observed behaviour of C_m . In order to overcome this flaw of the SK theory, we adopt the cluster formulation proposed by Soukoulis and Levin [23, 24]. In that proposal, starting from the Ising model, cluster of spins are used not only to provide intracusters short range spin correlations necessary to fit the experimental behavior of C_m but also to stabilize the SG state. It means that is possible to obtain a C_m curve with a broad maximum at a temperature above T_f . In the effective SG model which results from the cluster formulation, the quenched bond disorder appears as an intercluster interaction. Actually, one has two coupled problems. The first one refers to the intercluster disordered interaction which is solved exactly at mean field replica method since it is considered infinite ranged intercluster interaction. The second one refers to the intracuster problem. For this part, one should consider clusters with a certain inner structure. In fact, the intercluster contribution exhibits a cusp at T_f . However, as long as the intracuster contribution becomes dominant (by increasing the cluster size) the cusp tends to disappear and it appears a broad maximum located at a certain temperature which is higher than T_f in qualitative agreement with the experimental behaviour of C_m . Specifically for our case, it is used a cubic intracuster structure considering that an uniform ferromagnetic interaction is present between nearest neighbours and the RF acts in each spin. As a result, the intracuster Ising spin degrees of freedom of a finite cluster are computed by exact enumeration for each RF configuration. This crucial step allows, then, to go back to the intercluster problem, i. e. the SG problem, which is treated within the one-step replica symmetry breaking (RSB) scheme. In our work, there is no RSB without random bonds.

We highlight that in this cluster mean field theory for SG, we investigated in detail the roles of the intracuster and the intercluster parts to determine the behavior not only of C_m but also of χ_3 . As discussed previously,

² There is a clear disagreement for C_m between the experiment and the classical Monte Carlo results [19] even in zero H_t .

χ_3 has been in the center of intense debate which, ultimately, deals with the existence of the SG state in the $\text{LiHo}_x\text{Y}_{1-x}\text{F}_4$. In particular, there are also issues concerning the presence of SG in uniform external magnetic field h . For instance, simulations on three-dimensional Ising SG model have pointed inconclusive results concerning the existence of SG state in presence of h [25, 26], while it is well established that mean-field studies found SG state by means of the Almeida and Thouless analysis (λ_{AT}), in the so called RSB picture. In the present study, we shall demonstrate that it is still preserved the relationship $\chi_3 \sim \lambda_{\text{AT}}^{-1}$ in the cluster formulation without RF. In the presence of RF, that relationship is modified. As a consequence, one can expect that shall emerge three energy scales: (i) the RSB freezing temperature T_f ; (ii) T^* associated with the rounded maximum of χ_3 and (iii) T^{**} associated with the broad maximum of C_m . It should be noticed that T^* would exist only for finite RF. Actually, the central question of the present work is how T_f , T^* and T^{**} evolve as the RF effects are enhanced. Indeed, the behavior of T^* and T^{**} would indicate how the paramagnetic (PM) phase is unfolded in PM sub-regions displaying distinct spin correlations.

This paper is structured as follows. In Sec. II we discuss the model and the analytic calculations to get the order parameters and thermodynamic quantities as χ_3 and C_v . Our numerical results are presented in Sec. III. In Sec. IV we present the conclusion.

II. MODEL

We follow closely the cluster SG mean field theory proposed in Ref. [23] rewriting the Ising model with RFs, $H = -\sum_{i,j}^N J_{ij}\sigma_i\sigma_j - \sum_{i=1}^N h_i\sigma_i$, in terms of N_{cl} spin clusters with n_s spins inside of the ν -th cluster, hence $N = N_{cl}n_s$. This procedure defines a new variable $\sigma_\nu = \sum_i^{n_s} \sigma_{\nu,i}$ and the effective hamiltonian becomes

$$H = -\sum_{\nu < \lambda} J_{\nu\lambda}\sigma_\nu\sigma_\lambda - \sum_{\nu} \left(\sum_{i < j} J_1\sigma_{\nu,i}\sigma_{\nu,j} + \sum_i h_{\nu,i}\sigma_{\nu,i} \right). \quad (1)$$

At this stage, the only approximation is to consider that the clusters are separated by a distance far larger than their average size. Thus, the intercluster interaction is assumed to be independent of the site position inside the cluster [24]. It means that the neighboring clusters interact only via exchange interactions $J_{\nu\lambda}$ between total spins on each cluster with intracenter short-range interactions J_1 . In the model (1), the two sources of disorders $J_{\nu\lambda}$ and random fields h_i follow the probability distributions given below

$$P(J_{\nu\lambda}) = \frac{1}{\sqrt{2\pi \frac{J^2}{N_{cl}}}} \exp \left[-\frac{1}{2} \left(\frac{J_{\nu\lambda}}{\frac{J}{\sqrt{N_{cl}}}} \right)^2 \right] \quad (2)$$

and

$$\overline{P}(h_{\nu_i}) = \frac{1}{\sqrt{2\pi\Delta^2}} \exp \left[-\frac{1}{2} \left(\frac{h_{\nu_i}}{\Delta} \right)^2 \right]. \quad (3)$$

We use the same procedure as in Ref. [15] to obtain the free energy per cluster $f = -1/(\beta N_{cl}) \langle \ln Z(\{J_{ij}\}, \{h_i\}) \rangle_{J,h}$, where $Z(\{J_{ij}\}, \{h_i\})$ is the partition function for a given quenched distribution of the random couplings and fields. $\langle \dots \rangle_{J,h}$ denotes averages over these disorders and $\beta = 1/T$. As usual, the replica method is applied in order to calculate the quenched disorders:

$$-\beta f = \lim_{n \rightarrow 0} \frac{1}{N_{cl}n} (\langle \langle Z(\{J_{ij}\}, \{h_i\})^n \rangle \rangle_{J,h} - 1). \quad (4)$$

The average over the random couplings can be evaluated and the replicated partition function for a given distribution of RF is expressed as

$$\langle \langle Z(\{h_i\})^n \rangle \rangle = \left\langle \text{Tr} \exp \left[-\beta \sum_{\nu} \sum_{\alpha} H_{\text{intra}}^{\alpha}(\nu, \{h_i\}) + \frac{\beta^2 J^2}{4N_{cl}} \sum_{\alpha, \gamma} \left(\sum_{\nu} \sigma_{\nu}^{\alpha} \sigma_{\nu}^{\gamma} \right)^2 \right] \right\rangle_{h_i}, \quad (5)$$

where Tr is the trace over spin variable, α and γ are the replica indices with the $\sum_{\alpha, \gamma}$ considering α and $\gamma = 1, \dots, n$, $\langle \dots \rangle_{h_i}$ denotes the average over the RF distribution, and $H_{\text{intra}}^{\alpha}(\nu, \{h_i\}) = -\sum_{i < j} J_1 \sigma_{\nu,i}^{\alpha} \sigma_{\nu,j}^{\alpha} - \sum_i h_{\nu,i} \sigma_{\nu,i}^{\alpha}$ is represents the intracenter terms. The quadratic terms are linearized by introducing the SG order parameters:

$$\langle Z(\{h_i\})^n \rangle = \int Dq_{\alpha, \gamma} \exp \left\{ -N_{cl} \left[\frac{\beta^2 J^2}{4} \sum_{\alpha, \gamma} q_{\alpha, \gamma}^2 - \frac{1}{N_{cl}} \left\langle \ln \text{Tr} \exp [-\beta \sum_{\nu} H_{\text{eff}}(\nu, \{h_i\})] \right\rangle_{h_i} \right] \right\} \quad (6)$$

where

$$H_{\text{eff}}(\nu, \{h_i\}) = \sum_{\alpha} H_{\text{intra}}^{\alpha}(\nu, \{h_i\}) - \frac{\beta J^2}{2} \sum_{\alpha, \gamma} q_{\alpha \gamma} \sigma_{\nu}^{\alpha} \sigma_{\nu}^{\gamma} \quad (7)$$

is an effective single-cluster model with interacting replicas. In the thermodynamic limit, the functional integrals over $q_{\alpha \gamma}$ are obtained from the saddle-point method:

$$q_{\alpha \gamma} = \left\langle \frac{\text{Tr} \sigma^{\alpha} \sigma^{\gamma} \exp [-\beta H_{\text{eff}}(\{h_i\})]}{\text{Tr} \exp [-\beta H_{\text{eff}}(\{h_i\})]} \right\rangle_{h_i}, \quad (8)$$

in which this correlation for the same replica ($\alpha = \gamma$) can be associated with the expectation value of the cluster magnetic moment magnitude, while for different replicas ($\alpha \neq \gamma$) it is related to the SG order parameter.

The one-step replica symmetry breaking 1S-RSB is used to parametrize the replica matrix as: $\bar{q} = q_{\alpha\alpha}$, $q_0 = q_{\alpha\gamma}$ if $I(\alpha/x) = I(\gamma/x)$ or $q_1 = q_{\alpha\gamma}$ if $I(\alpha/x) \neq I(\gamma/x)$, where $I(y)$ is the smallest integer greater than y and x is the size of diagonal blocks of the replica matrix with 1S-RSB solution [13]. This ansatz results in the following free energy expression

$$\beta f = \frac{J^2 \beta^2}{4} (\bar{q}^2 + x(q_1^2 - q_0^2) - q_1^2) - \frac{1}{x} \left\langle \int Dz \ln \int Dv [K(\{h_i\}, v, z)]^x \right\rangle_{h_i} \quad (9)$$

with $\int D\xi = \int d\xi e^{-\xi^2/2}/\sqrt{2\pi}$ ($\xi = z$ or v),

$$K(\{h_i\}, v, z) = \text{Tr} \exp[-\beta H_{\text{eff}}^{\text{1S}}(\{h_i\}, v, z)] \quad (10)$$

and the effective single-cluster model

$$H_{\text{eff}}^{\text{1S}}(\{h_i\}, v, z) = -(J\sqrt{q_1 - q_0}v + J\sqrt{q_0}z)\sigma - \frac{\beta J^2}{2}(\bar{q} - q_1)\sigma^2 - \sum_{i,j}^{n_s} J_1 \sigma_i \sigma_j - \sum_i^{n_s} h_i \sigma_i, \quad (11)$$

where the order parameters are exhibited in appendix A.

Other thermodynamic quantities can now be obtained from the free energy. For instance, the linear susceptibility χ_1 is given by $\chi_1 = \beta[\bar{q} - q_1 + x(q_1 - q_0)]$ [14]. The nonlinear susceptibility χ_3 can be derived from $\chi_3 = -\frac{1}{3!} \frac{\partial^2 \chi_1}{\partial h^2} \big|_{h \rightarrow 0}$, where h is an applied longitudinal magnetic field. The internal energy ($u = -\frac{\partial}{\partial \beta}(\beta f)$) and the specific heat ($C_m = \frac{d}{dT}u$) are also obtained:

$$C_m = C_{\text{inter}} + C_{\text{intra}} + C_{\text{RF}} \quad (12)$$

where

$$C_{\text{inter}} = \frac{d}{dT} \left[\frac{\beta J^2}{2} (\bar{q}^2 + x(q_1^2 - q_0^2) - q_1^2) \right], \quad (13)$$

$$C_{\text{intra}} = J_1 \frac{d}{dT} \left\langle \int Dz \frac{\int Dv K^{x-1} \text{Tr} \sum_{(i,j)}^{n_s} \sigma_i \sigma_j e^{-\beta H_{\text{eff}}^{\text{1S}}}}{\int Dv K^x} \right\rangle_{h_i}, \quad (14)$$

$$C_{\text{RF}} = \frac{d}{dT} \left\langle \int Dz \frac{\int Dv K^{x-1} \text{Tr} \sum_i^{n_s} h_i \sigma_i e^{-\beta H_{\text{eff}}^{\text{1S}}}}{\int Dv K^x} \right\rangle_{h_i}. \quad (15)$$

In particular, the replica symmetry solution can occur at high temperatures when $q = q_0 = q_1$, resulting in the following effective model

$$H_{\text{eff}}^{\text{RS}}(\{h_i\}) = -J\sqrt{q}z\sigma - \frac{\beta J^2}{2}(\bar{q} - q)\sigma^2 - H_{\text{intra}}(\{h_i\}). \quad (16)$$

The stability of the RS solution can be obtained from the de Almeida-Thouless eigenvalue [27] given by Eq. (B2).

The nonlinear susceptibility χ_3 is obtained within the RS solution from:

$$\chi_3 = \frac{1}{3!} \frac{d^3 m(q, \bar{q}, h)}{dh^3} \bigg|_{h=0}, \quad (17)$$

where

$$m(q, \bar{q}, h) = \left\langle \int Dz \frac{\text{Tr} \sigma \exp(-\beta H_{\text{eff}}^{\text{RS}}(\{h_i\}))}{\text{Tr} \exp(-\beta H_{\text{eff}}^{\text{RS}}(\{h_i\}))} \right\rangle_{h_i} \quad (18)$$

In Appendix C, we develop an explicit form for χ_3 in terms of spin correlations which is given in Eq. (C5). This form can also be expressed directly in terms of λ_{AT} (see Appendix B) as

$$\chi_3 = \frac{\beta^3}{3} \left[\frac{3}{b(\lambda_{\text{AT}})} - 1 \right] V_2 \quad (19)$$

where $b(\lambda_{\text{AT}}) = (2 - \beta^2 J^2 V_3)(\lambda_{\text{AT}} - V_5) - \beta^4 J^4 V_2 V_4$ with

$$V_2 = \left\langle \int Dz [\langle \sigma^4 \rangle - 4\langle \sigma \rangle \langle \sigma^3 \rangle - 3\langle \sigma^2 \rangle^2 + 12\langle \sigma \rangle^2 \langle \sigma^2 \rangle - 6\langle \sigma \rangle^4] \right\rangle_{h_i}, \quad (20)$$

$$V_3 = \left\langle \int Dz [\langle \sigma^4 \rangle - 2\langle \sigma \rangle \langle \sigma^3 \rangle - \langle \sigma^2 \rangle^2 + 2\langle \sigma \rangle^2 \langle \sigma^2 \rangle] \right\rangle_{h_i}, \quad (21)$$

$$V_4 = \left\langle \int Dz [\langle \sigma \rangle \langle \sigma^3 \rangle - \langle \sigma \rangle^2 \langle \sigma^2 \rangle] \right\rangle_{h_i} \quad (22)$$

and

$$V_5 = \beta^2 J^2 \left\langle \int Dz [\langle \sigma \rangle \langle \sigma^3 \rangle - 3\langle \sigma \rangle^2 \langle \sigma^2 \rangle + 2\langle \sigma \rangle^4] \right\rangle_{h_i}, \quad (23)$$

in which $\langle \dots \rangle$ represents the thermal average over the effective RS model $H_{\text{eff}}^{\text{RS}}$ with $h = 0$. Particularly, in absence of RF and for $T \geq T_f$ ($q = 0$ with RS stable), we obtain $V_4 = 0$ and $V_5 = 0$, resulting in

$$\chi_3(\Delta = 0) = \frac{\beta^3}{3} \left[\frac{3}{(2 - \beta^2 J^2 V_3)\lambda_{\text{AT}}} - 1 \right] V_2 \quad (24)$$

Therefore, the χ_3 diverges at T_f in which $\lambda_{\text{AT}} = 0$.

III. RESULTS

In this section, we present numerical results obtained from the single-cluster problem (Eqs. (9)-(11)). The behavior of the SG order parameters, linear χ_1 and nonlinear χ_3 susceptibilities, and specific heat C_m are analyzed considering combined variations of the parameters Δ/J , J_1/J and T/J for clusters following a simple cubic lattice shape with 8 spins. In particular, the 1S-RSB and the

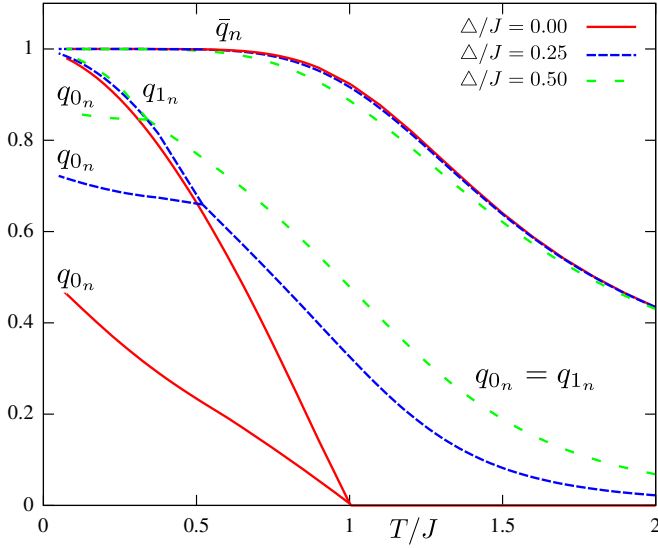


FIG. 1. Normalized one step RSB order parameters as a function of the temperature for several values of Δ when $J_1/J = 0.70$ and eight spins per cluster $n_s = 8$ assuming a simple cubic lattice shape. Here, $q_{0n} = q_0/n_s^2$, $q_{1n} = q_1/n_s^2$ and $\bar{q}_n = \bar{q}/n_s^2$.

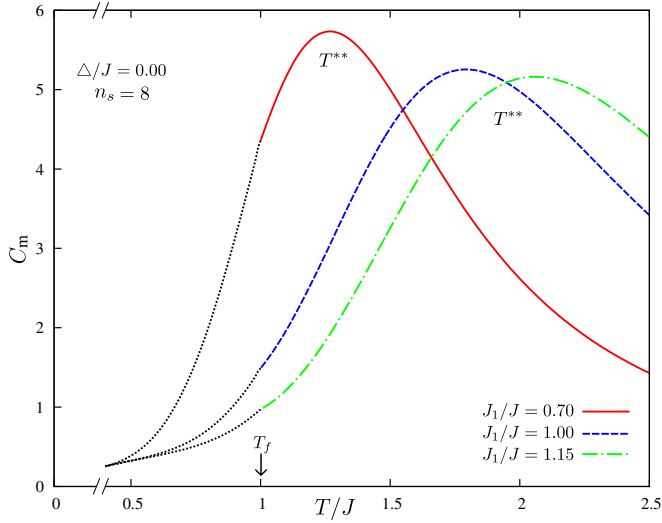


FIG. 2. Specific heat as a function of temperature for different ferromagnetic intracluster interactions without the presence of RF. The dotted lines represent results of unstable RS solution ($\lambda_{AT} < 0$). The C_m values located below the axis break are not significant and numerically reliable.

replica symmetry stability (de Almeida-Thouless (AT) line) are used in order to locate the freezing temperature T_f .

Fig. 1 shows the 1S-RSB SG order parameters as a function of the temperature. For instance, q_0 and q_1 exhibit a transition from the RS behavior ($q = q_0 = q_1$) to a RSB region ($q_0 \neq q_1$) at the freezing temperature T_f . The RFs induce these order parameters even in the RS region. In addition, the RFs displace the T_f to lower tem-

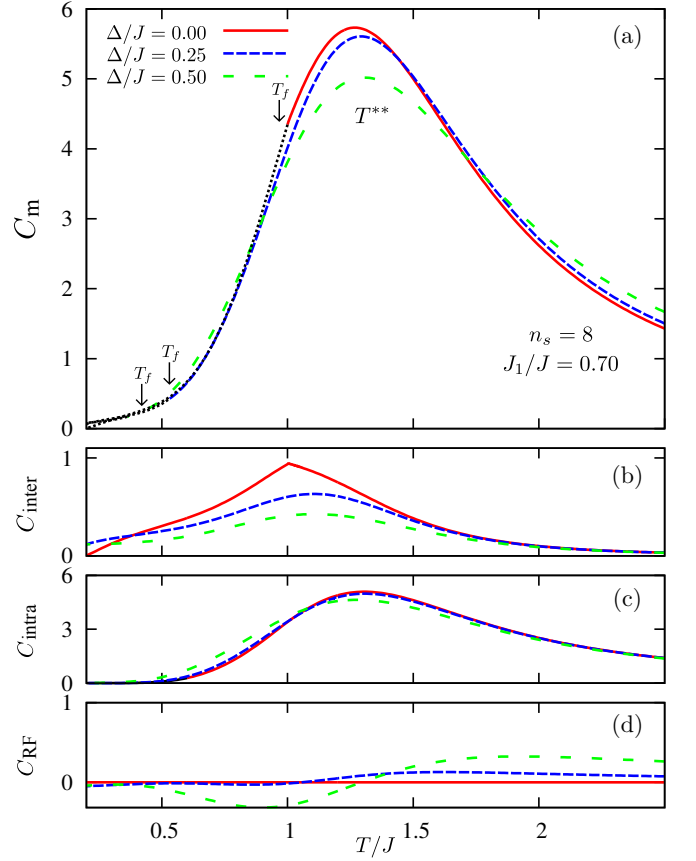


FIG. 3. (a) C_m versus T/J different values of Δ (0.00, 0.25 J and 0.50 J) when $J_1/J = 0.70$ is keeping constant for simple cubic lattice clusters with 8 spins. Panels (b), (c) and (d) show the contributions from intercluster and intracluster interactions, and the explicit RF effects for the specific heat, respectively (see Eqs. (13), (14) and (15)).

peratures. In particular, the transition from RS to RSB solution can also be located by the Almeida-Thouless line that coincides with the beginning of the RSB. Furthermore, in the present cluster formalism, the replica diagonal elements have an essential role. They are represented by $\bar{q} = \langle \sigma_v^2 \rangle_{H_{eff}}$ that can be interpreted as the intensity of the cluster magnetic moment [23]. That is an important difference with Ref. [12]. There, using the SK model, $\bar{q} = 1$. Here, \bar{q} depends on the temperature as well as the intracluster interactions and RFs.

The specific heat and susceptibilities are now analyzed in order to understand the effects of RFs on this SG problem. For instance, Fig. 2 exhibits the C_m as a function of T/J for different intracluster interactions in absence of RF ($\Delta = 0$). The C_m curve presents a broad maximum at a temperature T^{**} that depends on the intensity of J_1 (see Fig. 2). The increase of J_1 displaces T^{**} to higher temperatures at the same time that the C_m maximum becomes lower. It means that the intracluster short-range interactions affect the specific heat behavior. At T_f the C_m presents a small mark that is associated with the in-

tercluster interactions. Specifically, this comes from the temperature derivative of the SG order parameters (see Eq. 13) that become different from zero at T_f (see Fig. 1 for $\Delta = 0$). It is also important to note that T_f/J is keeping at unity and the maximum appears in a range of stable RS solution ($\lambda_{AT} > 0$). In other words, $T_f < T^{**}$ and the ratio T^{**}/T_f can be adjusted by J_1/J in order to get the behavior observed in canonical SG systems ($T^{**}/T_f \approx 1.30$), as instance $J_1/J = 0.70$.

However, the presence of RFs changes this scenario. As shown in Fig. 3(a), the C_m still exhibits the broad maximum at T^{**} that is weakly dependent on Δ , but T_f is decreased by RFs. As a consequence, T^{**}/T_f grows when the RFs are considered. The different contributions for C_m can be analyzed in Figs. 3(b)-3(d). For instance, the intercluster interaction contributions displayed in panel (b) indicate that the peak at T_f vanishes in the presence of RFs. This occurs because the RF induces the SG order parameters at the whole range of temperature, avoiding the discontinuity in the derivative of these order parameters as discussed before. As a consequence, the C_m curve becomes smooth at T_f (see Fig. 3(b)). From the Fig. 3(c), one can see that the short-range intracluster represents the main contribution for C_m . This contribution is weakly affected by the RF, at least in the range of low strength of RF adopted here. This explains why the T^{**} position is slightly dependent on the RFs. Besides, the explicit RF contribution (Fig. 3(d)) has a lower intensity as compared with the intracluster one.

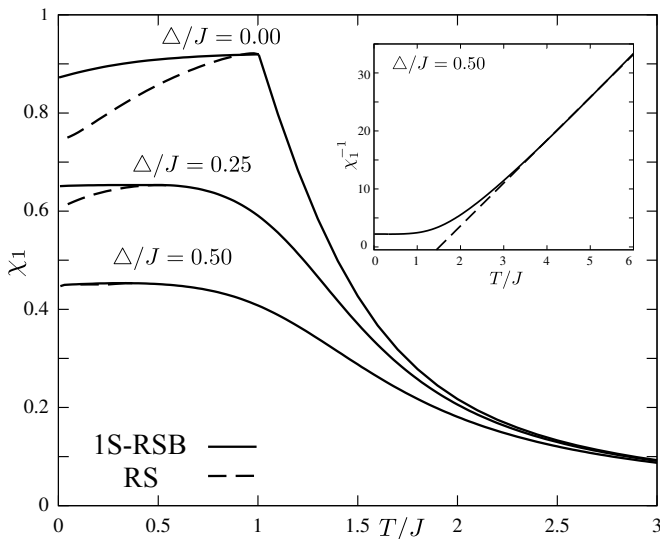


FIG. 4. Linear susceptibility χ_1 vs T/J for $J_1/J = 0.70$ and $n_s = 8$ with $\Delta/J = 0.00, 0.25$ and 0.50 . The solid and dashed lines correspond to 1S-RSB and RS solutions respectively. The detail presents χ_1^{-1} as a function of T/J (full line) when $\Delta/J = 0.50$. The dashed line represents the Curie-Weiss law linear extrapolation from higher temperatures.

The linear susceptibility can be analyzed in Fig. 4. For the absence of RF, χ_1 presents a cusp at the freezing temperature, in which the χ_1 becomes weakly dependent

on the temperature within the RSB region, appearing a divergence between the results obtained with RS and 1S-RSB solutions. However, this cusp is suppressed in the presence of RF, but the divergence between both solutions is still present with a weak dependence on the temperature for the 1S-RSB. In addition, the detail of Fig. 4 exhibits the reciprocal of χ_1 that follows a Curie-Weiss behavior at higher temperatures ($T/J \gtrsim 3T_f/J$).

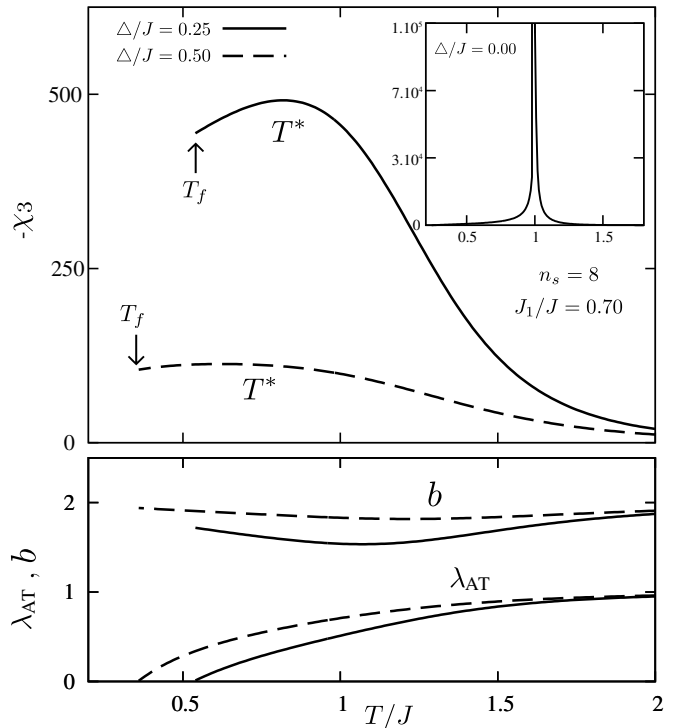


FIG. 5. (a) Nonlinear susceptibility χ_3 vs T/J for intracluster interaction $J_1/J = 0.70$ with $\Delta/J = 0.25$ and 0.50 . The arrows locate the limit of RS stable solution. The inset shows the χ_3 vs T/J for $\Delta/J = 0.00$. Panel (b) presents the behavior of λ_{AT} and the denominator b of the χ_3 expression for $\Delta > 0$.

Another relevant result can be derived from the higher order susceptibility terms that are more sensitive to the SG phase transition. For instance, Fig. 5(a) displays the nonlinear susceptibility χ_3 as a function of T/J for clusters with $n_s = 8$ and $J_1 = 0.70$ when different values of Δ are considered. The χ_3 result for $\Delta = 0$ shows a divergence at the freezing temperature T_f (see inset of Fig. 5(a)), identifying the SG phase transition in absence of RF. However, this divergent peak becomes a rounded maximum at a temperature T^* as Δ increases. In particular, T^* does not match anymore with the transition temperature T_f as can be seen Fig. 5(b) from the λ_{AT} curve. It is important to remark that, in this case, T^* occurs in a range of temperature where the RS solution is stable, i.e. $T_f < T^*$ for a given Δ . It also means that the temperature indicated by T^* in the presence of RF does not locate an SG phase transition. This T^* displacing from T_f can be better understood by analyzing the χ_3 denominator b (see Eq. 19) in Fig. 5(b). In con-

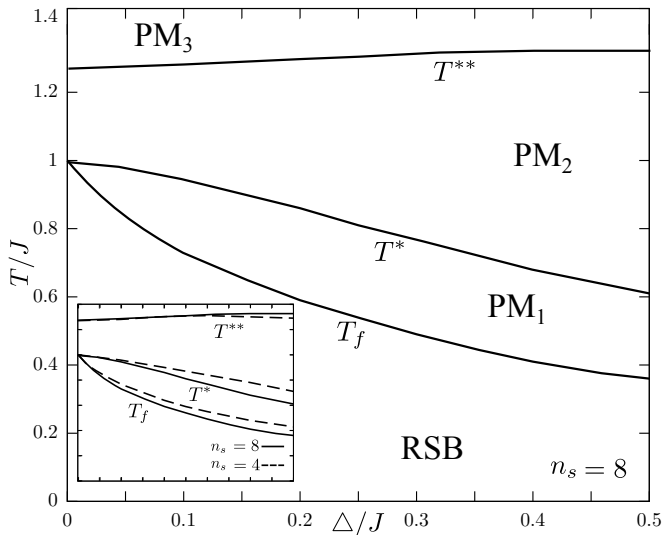


FIG. 6. Phase diagram T/J vs Δ for $n_s = 8$ and $J_1/J = 0.70$ that shows T_f separating the RSB solution (an SG state) from the RS PM phases. The figure also displays the crossover temperatures T^{**} and T^* delimiting the different PM behaviors (PM₁, PM₂ and PM₃) associated with C_m and χ_3 maximum respectively. The inset exhibits a comparison between results obtained from $n_s = 4$ and $n_s = 8$, where no significant changes are observed.

trast to the case with $\Delta = 0$, where $b = \lambda_{AT}$, b is always positive when $\Delta > 0$. In this particular, b presents a smooth minimum around the temperature T^* , leading to the rounding of χ_3 , whereas λ_{AT} becomes zero at a lower temperature. Therefore, different from the $\Delta = 0$ result, T^* can identify a crossover between PM phases. This unexpected behavior is associated with RF effects.

These results for the behavior of T_f , T^* and T^{**} can be better explored in the phase diagram of Fig. 6. First of all, there are two distinct regions: one with stable RS solution ($T > T_f$) and another with RSB ($T < T_f$). More important, T^* and T^{**} are located within the RS regime, in which PM phases occur with different characteristics. For higher temperatures ($T > T^{**}$), the PM phase follows the Curie-Weiss law, in which the reciprocal of the linear susceptibility presented in the inset of Fig. 4 shows a linear extrapolation (dashed line) from high temperatures. As the temperature decreases, the short-range ferromagnetic interactions become more relevant introducing local ferromagnetic correlations. These correlations enhance the cluster magnetic moment (\bar{q}), without bringing a long-range order due to the absence of FE intercluster interactions [28]. Although, this mechanism is not able to bring a phase transition, the specific heat exhibits a maximum at T^{**} , where these ferromagnetic correlations turn important. In other words, some of the cluster inner degrees of freedom are frozen around T^{**} favoring the stabilization of small ferromagnetic clusters. Moreover, the intercluster disordered interactions act on the cluster magnetic moments that are still thermal fluc-

tuating. Indeed, these fluctuations become progressively slower below T^* until the RSB SG transition at T_f . It means that we can find more two other kinds of PM phase: one between T^{**} and T^* , and another between T^* and T_f .

IV. CONCLUSION

In this work, we have analyzed the behavior of C_m and χ_3 in a Ising SG model formulated in terms of spin clusters with a RF following a Gaussian distribution with width Δ . The cluster formulation results in two coupled problems: (i) the intercluster one, solved exactly at mean field level; (ii) the intracluster one, understood as the intracluster interaction plus the inner cluster magnetic site structure, solved exactly.

Our main results on C_m and χ_3 are summarized in the phase diagram in Fig. (6). The smooth maximum of C_m at T^{**} and the increasingly rounded maximum of χ_3 at T^* lead the PM phase to be unfolded in three regions: PM₃ for $T > T^{**}$, PM₂ for $T^{**} < T < T^*$ and PM₁ for $T_f < T < T^*$. It should be remarked that T_f and T^* decrease whereas T^{**} is weakly affected as Δ/J enhances. That behavior is responsible by the enlargement of the PM₂ region. We also remark two aspects: (i) the rounded maximum of χ_3 is no longer related with the onset of SG state; (ii) the nontrivial broken ergodicity corresponding to the onset of RSB SG state at T_f is still given by the AT line ($\lambda_{AT} = 0$) for any value of Δ/J .

The unfolding of the PM phase suggests that spin correlations develop in three stages as the temperature is lowered from the conventional high temperature paramagnetism (called here PM₃) until the RSB SG transition at T_f . In absence of RF, we choose $T_f \simeq 1.3T^{**}$ by adjusting the ferromagnetic intracluster interaction. The smooth maximum of C_m at T^{**} indicates that the intracluster ferromagnetic interaction starts to overcome thermal fluctuations selecting magnetic global states of the cluster, which form small ordered ferromagnetic regions. This development is illustrated by the behavior of the intensity of the cluster magnetic moment \bar{q} as the temperature is lowered (see Fig. (1)). Indeed, the growth of \bar{q} towards its maximum value favors the nontrivial broken ergodicity at T_f for $\Delta = 0$. However, when Δ/J enhances, T^{**} and T_f strongly deviate from the relationship $T^{**} \simeq 1.3T_f$. Thereby, the small ferromagnetic spin clusters formation becomes increasingly far above T_f . In particular, the mentioned deviation is mainly caused by the behavior of T_f which is quite affected by the RF. That is not the case for T^{**} , at least, for the range of Δ/J used in our calculations ($0 \leq \Delta/J \leq 0.5$). In addition, as the divergence in χ_3 becomes rounded at T^* , there is the onset of the PM₁ region. This temperature is also affected by the RF. Remarkably, although the RF couples with individual spins, our results show that it is the small ferromagnetic spin clusters which play the important role to determine the rounded maximum of χ_3 and the RSB

SG instability. In fact, \bar{q} already has its maximum value at T_f and, mostly important, very close to its maximum value at T^* . This particular point suggests that the spin dynamics in the PM_1 region is rather non-trivial. Quite probably, a very slow one. Thus, one can expect that in PM_1 region there is a slow growth of free-energy barriers before the nontrivial broken ergodicity at T_f . In that sense, T^* would be a crossover temperature between two types of spin dynamics.

Since we provide an unified description of the C_m and χ_3 with a RF, we believe that some results discussed above can have relevance for the $\text{LiHo}_x\text{Y}_{1-x}\text{F}_4$ compound when the applied transverse field H_t is weak ($H_t < 0.5T$) assuming that the RF is induced by H_t [7, 8]. Our proposal is that in the $\text{LiHo}_x\text{Y}_{1-x}\text{F}_4$, the paramagnetic phase is unfolded in three regions with one of them (the PM_2 region) being a region dominated by spin short range correlations favoring clusters formation and other of them (the PM_1 region) acting as precursor of RSB SG that appears at lower temperatures. We remark that our results reproduce qualitatively not only the replacement of the divergence in χ_3 by a rounded maximum located at T^* but also the decreasing of T^* as H_t is increased, which are observed for small Ho concentration in the **LiHo_xY_{1-x}F₄** compound for $H_t < 0.2T$ (see Ref. [1]). Besides the existence of RSB SG state at lower temperature, our results also show a presence of a broad maximum located at T^{**} as usually observed in SG systems. However, it is also predicted an increasingly deviation of the relationship between the freezing temperature T_f and T^{**} , as well between T^* and T^{**} as H_t is increased. This deviation between T^* and T^{**} could signalize the interplay between the RF induced by H_t and small ferromagnetic spin clusters as discussed in the present work. In fact, the deviation of the conventional relationship between T^{**} and T_f has been observed for $x = 0.018, 0.045$ and 0.08 , but, in absence of H_t [22]. Lastly, the nature of PM_1 region as described above may suggest a Griffiths phase as precursor of the RSB SG state as proposed by Biltmo and Henelius for $\text{LiHo}_x\text{Y}_{1-x}\text{F}_4$ [19]. One interesting question is how robust our results are in the quantum limit, i. e., for strong H_t . This limit is currently been analyzed by us.

ACKNOWLEDGMENTS

This study was financed in part by the Coordenação de Aperfeiçoamento de Pessoal de Nível Superior - Brazil (CAPES) - Finance Code 001, and Conselho Nacional de Desenvolvimento Científico e Tecnológico (CNPq).

Appendix A

The 1S-RSB parameters q_0 , q_1 , \bar{q} and x are obtained by extremizing the free energy (9):

$$\bar{q} = \left\langle \int Dz \frac{\int Dv K^{x-1} \text{Tr} \sigma^2 \exp(-\beta H_{\text{eff}}^{\text{1S}})}{\int Dv K^x} \right\rangle_{h_i} \quad (\text{A1})$$

$$q_0 = \left\langle \int Dz \left[\frac{\int Dv K^{x-1} \text{Tr} \sigma \exp(-\beta H_{\text{eff}}^{\text{1S}})}{\int Dv K^x} \right]^2 \right\rangle_{h_i} \quad (\text{A2})$$

$$q_1 = \left\langle \int Dz \frac{\int Dv K^{x-2} [\text{Tr} \sigma \exp(-\beta H_{\text{eff}}^{\text{1S}})]^2}{\int Dv K^x} \right\rangle_{h_i} \quad (\text{A3})$$

and

$$\frac{x^2}{4} (q_1^2 - q_0^2) = \left\langle \int Dz \left[\frac{\int Dv K^x \ln K^x}{\beta^2 J^2 \int Dv K^x} - \frac{\int Dv \ln K}{\beta^2 J^2} \right] \right\rangle_{h_i} \quad (\text{A4})$$

where the K and $H_{\text{eff}}^{\text{1S}}$ dependence on $(\{h_i\}, v, z)$ is suppressed in order to brief the equations.

Appendix B

The stability analysis of the RS solution follows close to de AlmeidaThouless calculation [27]. However, here, the Hessian matrix have also to consider explicitly the fluctuations on the replica diagonal elements. In this case, the replicon eigenvalue is given by the correlations:

$$\lambda_{\text{AT}} = 1 - \beta^2 J^2 [\langle \langle \sigma^\alpha \sigma^\gamma \sigma^\alpha \sigma^\gamma \rangle \rangle_{h_i} - 2 \langle \langle \sigma^\alpha \sigma^\gamma \sigma^\alpha \sigma^\zeta \rangle \rangle_{h_i} + \langle \langle \sigma^\alpha \sigma^\gamma \sigma^\delta \sigma^\zeta \rangle \rangle_{h_i}] \quad (\text{B1})$$

in which $\langle \langle \dots \rangle \rangle_{h_i} \equiv \left\langle \frac{\text{Tr} \dots \exp[-\beta H_{\text{eff}}(\{h_i\})]}{\text{Tr} \exp[-\beta H_{\text{eff}}(\{h_i\})]} \right\rangle_{h_i}$ and the labels $\{\alpha, \gamma, \delta, \zeta\}$ are replica indices. In particular, these replica spin correlations result in

$$\lambda_{\text{AT}} = 1 - J^2 \beta^2 \left\langle \int Dz (\langle \sigma \sigma \rangle_{H_{\text{eff}}^{\text{RS}}} - \langle \sigma \rangle_{H_{\text{eff}}^{\text{RS}}}^2)^2 \right\rangle_{h_i}, \quad (\text{B2})$$

where $\langle \dots \rangle_{H_{\text{eff}}^{\text{RS}}} = \text{Tr} \dots \exp[-\beta H_{\text{eff}}^{\text{RS}}] / \text{Tr} \exp[-\beta H_{\text{eff}}^{\text{RS}}]$ with $H_{\text{eff}}^{\text{RS}}$ defined in Eq. (16).

Appendix C

In order to obtain χ_3 within the RS solution, the explicitly dependence of q and \bar{q} on h have to be considered in Eqs (17)-(18). We expand q and \bar{q} up to second order in h : $q = q_0 + q_2 h^2 + O(h^4)$ and $\bar{q} = \bar{q}_0 + \bar{q}_2 h^2 + O(h^4)$. This derivation is a tedious but straightforward calculation that results in

$$\chi_3 = \frac{\beta^3 J^2}{3} \left[\left(\frac{1}{\beta^2 J^2} + V_3 \right) (\bar{q}_2 - q_2) + q_2 V_2 \right] \quad (\text{C1})$$

where

$$\bar{q}_2 - q_2 = \frac{\beta^2 + \beta^2 J^2}{2 - \beta^2 J^2 V_3} V_2, \quad (\text{C2})$$

$$q_2 = \frac{\beta^2 V_1}{2 - \beta^2 J^2 (V_1 + V_3)}, \quad (\text{C3})$$

with

$$V_1 = 0.5(2 - \beta^2 J^2 V_3)(V_3 - V_2) + \beta^2 J^2 V_2 V_4 \quad (\text{C4})$$

V_2 , V_3 and V_4 given, respectively, in Eqs. (20), (21) and (22).

The expression for χ_3 can be written in terms of V_1 , V_2 and V_3 as:

$$\chi_3 = \frac{\beta^3}{3} \frac{1 + \beta^2 J^2 (V_1 + V_3)}{[2 - \beta^2 J^2 (V_1 + V_3)]} V_2. \quad (\text{C5})$$

-
- [1] P. E. Jönsson, R. Mathieu, W. Wernsdorfer, A. M. Tkachuk, and B. Barbara, Phys. Rev. Lett. **98**, 256403 (2007).
 - [2] C. Ancona-Torres, D.M. Silevitch, G. Aeppli, and T.F. Rosenbaum, Phys. Rev. Lett. **101**, 057201 (2008).
 - [3] K. Binder and A. P. Young, Rev. Mod. Phys. **58**, 801 (1986).
 - [4] W. Wu, D. Bitko, T. F. Rosenbaum, and G. Aeppli, Phys. Rev. Lett. **71**, 1919 (1993).
 - [5] J. A. Mydosh, Rep. Prog. Phys. **78**, 052501 (2015).
 - [6] M. Gingras, P. Henelius, J. Phys: Conf. Ser. **320**, 012001 (2011).
 - [7] M. Schechter, N. Laflorencie, Phys. Rev. Lett. **97**, 137204 (2006).
 - [8] S.M. A. Tabei, M. J. P. Gingras, Y.-J. Kao, P. Stasiak and J.-Y. Fortin, Phys. Rev. Lett. **97**, 237203 (2006).
 - [9] S. G. Magalhaes, C. V. Morais, F. M. Zimmer, M. J. Lazo, and F. D. Nobre, Phys. Rev. B **95**, 064201 (2017).
 - [10] W. Wu, B. Ellman, T. F. Rosenbaum, G. Aeppli, D. H. Reich, Phys. Rev. Lett. **67**, 2076 (1991).
 - [11] P. B. Chakraborty, P. Henelius, H. Kjonsberg, A. W. Sandvik, S. M. Girvin, Phys. Rev. B **70**, 144411 (2004).
 - [12] C. V. Morais, F. M. Zimmer, M. J. Lazo, S. G. Magalhaes, and F. D. Nobre Phys. Rev. B **93**, 224206 (2016).
 - [13] G. Parisi, J. Phys. A **13**, 1101 (1980).
 - [14] G. Parisi, J. Phys. A **13**, 1887 (1980).
 - [15] R. F. Soares, F. D. Nobre and J. R. L. de Almeida, Phys. Rev. B **50**, 6151 (1994).
 - [16] D. Sherrington and S. Kirkpatrick, Phys. Rev. Lett. **35**, 1792 (1975).
 - [17] R. Pirc, B. Tadic, R. Blinc, Phys. Rev. B **36**, 8607 (1987).
 - [18] T. K. Kopec, B. Tadic, R. Pirc, R. Blinc, Z. Phys. B **78**, 493 (1990).
 - [19] A. Biltmo, P. Henelius, Nat. Comm. **3**, 857(2012).
 - [20] K. H. Fischer and J. A. Hertz, Spin Glasses (Cambridge University Press, Cambridge, England, 1991).
 - [21] S. Gosh, T. F. Rosenbaum, G. Aeppli, N. N. Copper-smith, Nature **425**, 48 (2003).
 - [22] J. A. Quilliam, C. G. A. Mugford, A. Gomez, S. W. Kycia, J. B. Kycia, Phys. Rev. Lett. **98**, 037203 (2007).
 - [23] C. M. Soukoulis, K. Levin, Phys. Rev. B, **18**, 1439 (1978).
 - [24] C. M. Soukoulis, Phys. Rev. B, **18**, 3757 (1978).
 - [25] M. Baity-Jesi, R. A. Baos, A. Cruz, L. A. Fernandez, J. M. Gil-Narvion, A. Gordillo-Guerrero, D. Iiguez, A. Maiorano, F. Mantovani, E. Marinari et al, Phys. Rev. E **89**, 032140 (2014).
 - [26] M. Baity-Jesi, R. A. Baos, A. Cruz, L. A. Fernandez, J. M. Gil-Narvion, A. Gordillo-Guerrero, D. Iiguez, A. Maiorano, F. Mantovani, E. Marinari et al, J. Stat. Mech. P05014 (2014).
 - [27] J. R. L. de Almeida, D. J. Thouless, J. Phys. A **11**, 983 (1978).
 - [28] F. M. Zimmer, M. Schmidt, S. G. Magalhaes, Phys. Rev. E **89**, 062117 (2014).